

NUMERICAL PREDICTION OF THE STRUT INTERFERENCE ON A REGIONAL AIRCRAFT WIND-TUNNEL MODEL

SERENA RUSSO¹, JÜRIG MÜLLER², NICOLA PALETTA³, STEPHAN ADDEN⁴ AND LUIS P. RUIZ-CALAVERA⁵

¹ Dream Innovation
via F. Parri 1 81030 Sant'Arpino (Caserta) – Italy
serena.russo@dreaminnovation.it – www.dreaminnovation.it

² RUAG Schweiz AG
Schiltwaldstrasse 6032 Emmen – Switzerland
juerg.mueller@ruag.com - www.ruag.com/en

³ IBK Innovation GmbH & Co. KG
Butendeichsweg 2 21129 Hamburg – Germany
nicola.paletta@ibk-tech.de - www.ibk-innovation.de/

⁴ IBK Innovation GmbH & Co. KG
Butendeichsweg 2 21129 Hamburg – Germany
stephan.adden@ibk-tech.de - www.ibk-innovation.de/

⁵ AIRBUS DEFENCE & SPACE
28906 Getafe (Madrid) – Spain
luis.ruiz@airbus.com – www.airbus.com

Key words: Strut Interference, CFD, regional aircraft.

Abstract. The aim of the work presented in this paper is to determine the aerodynamic interference effects of a typical strut supporting aircraft models during wind tunnel tests by means of steady RANS simulations of the flow field. Computational fluid dynamics simulations are performed to predict the interference produced by a strut having an elliptic shape. Two configurations of a scaled model of a regional aircraft are considered: a clean cruise configuration and a high-lift condition with a landing flap setting. In this paper only power-off conditions (i.e. without simulation of propeller effects) are considered. The strut effect is analyzed for several angles of incidence and sideslip. The flow field and forces disturbance caused by the strut are derived by comparing simulations with and without the support. The interference is analyzed in terms of global forces and moments coefficients in the body axes system. With this work, it is possible to derive an interpolation surface or a fitting surface from the numerical data that represents the difference between results with and without the strut, for each aerodynamic coefficient. These surfaces are important to study the variation of the interference with the angle of incidence and the angle of sideslip and, to perform corrections of the experimental wind tunnel data also in conditions that are not simulated in CFD.

1 INTRODUCTION

The aim of the work presented in this paper is to study the aerodynamic interference effects caused by a single strut supporting an aircraft model during wind tunnel tests. The flow field and forces distortion caused by the presence of the sting are derived from comparisons between simulations with and without the support. CFD simulations are used to evaluate the various bias present in the experimental wind tunnel data and to reduce the uncertainties related to the determination of the effects due to the presence of the support.

The wind tunnel model supports (struts) are designed to be as small as possible, under the constraint that they should sustain the forces generated by the model over a wide range of flow conditions. In addition, they must house instrumentation cabling and in the case of powered models route the required energy into the model. On the other hand, it is well known that their shape can strongly affect the aerodynamic flow field around the model with significant consequences on the accuracy of the measured data [3][4]. Several studies were undertaken in the past decades [5][6] to determine this effect for numerous configurations and flow velocity.

In most wind tunnel procedures, the strut effect is accounted for thanks to various corrections methods [7][8]. Unfortunately, the presently existing methods exhibit several drawbacks [9]:

- they differ from one wind tunnel to another, making it difficult to compare final results;
- they rely on simplifying hypotheses and/or empirical assumptions, which validity is doubtful for example at high Mach numbers or for unconventional models;
- they call upon dedicated experiments which are expensive and require the introduction of another support, i.e. additional distortions of the flow.

In order to alleviate these shortcomings, several recent [10][11] or older [12] initiatives aimed at determining whether advanced numerical simulations could help in understanding and predicting the support interference effect.

The objective of the current study is to predict the effects of a single-strut interference on all aerodynamic forces and moments on an Airbus Defence & Space configuration tested in the RUAG Large Low Speed Wind Tunnel Emmen in Switzerland (LWTE). Two configurations of a scaled model of a turboprop transport aircraft are considered: a clean configuration representative of a cruise condition and a high-lift configuration with extended flaps, namely landing. In this paper only power-off conditions (i.e. without simulation of propeller effects) are considered.

2 PROBLEM DESCRIPTION

Over the years, many test campaigns have been carried out in the RUAG wind tunnel at Emmen using a wide range of aircraft models and mounting systems. Depending on the aircraft geometry and support configuration tested, strut interference effects were shown to be potentially significant. These effects are normally determined by experimental means [13]. The results obtained serve as a basis for the determination of correction laws for a particular model and setup combination. However, testing other models requires the performance of new tests to derive accurate support effects. To avoid these expensive tests, CFD may be an appropriate alternative to predict these support effects. The work undertaken and reported in

this paper aims at validating the ability of RANS CFD tools to predict the effect of a single strut on the global aerodynamic forces acting on the model.

The Airbus model is tested in the RUAG wind tunnel (LWTE) [14]. It is equipped with an internal strain gauge balance which measures the six forces and moments and is mounted on a single ventral strut having an elliptical section. The size of the test section is 7.0x5.0 m, the frontal area of the strut is about $1 \times 10^{-3} m^2$ and the span of the model is 3.0 m. The hydraulic diameter of the fuselage is 0.337 m, i.e. the ratio of the minimum strut diameter to the fuselage diameter is 0.31, which should yield moderate disturbance according to [15].

Figure 1 shows the model as mounted on the elliptic strut in the LWTE test section. The whole campaign is performed at a Mach number of 0.20 and a Reynolds number of 1.3×10^6 based on mean aerodynamic chord.

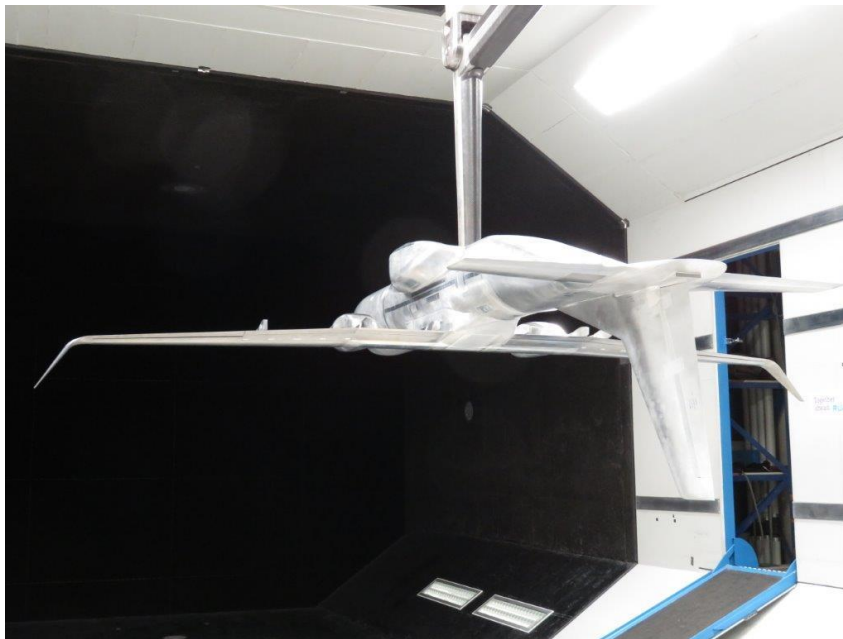


Figure 1: Airbus model during test with ventral strut at LWTE

3 NUMERICAL SIMULATION APPROACH

3.1 Flow solver

The Reynolds-averaged Navier-Stokes (RANS) equations are solved using a commercial CFD code (FLUENT [16]). An implicit, upwind, second-order accurate density-based solver [16] is selected. The two-equation $k-\epsilon$ turbulence model is employed by integrating to the wall (i.e., without using wall functions) and fully turbulent flow is assumed. The problem is solved using a second-order discretization scheme initially with a CFL number of 1.0 to converge the steady-state iterative residuals by 3 orders of magnitude and, then, a CFL number between 5 and 10 is used. After performing an iterative error analysis, the final normalized steady-state residual tolerance criteria used in this study is a 6 order of magnitude reduction (10^{-6}).

3.2 Grid generation

ICEM [17], a commercial grid generation tool, is used to generate the flow field mesh. The mesh for 3-D flow solutions has both structured (hexahedral) and unstructured (pyramidal and tetrahedral) cells. The structured grid is used to capture the gradients and resolve the boundary layer near the surface of the aircraft model. The rest of the domain has a mixture of unstructured grid blocks.

The total number of cells is between 8 and 10 millions for both configurations with and without the strut. For computations without the strut, new blocks of mesh are added to fill in the volume of the strut, so that no alteration is made to the other parts of the mesh. The whole domain is divided into two parts: a volume closer to the model (called internal domain) and a far field volume (called external domain). The first domain is the same for all the possible conditions in terms of angle of incidence and angle of sideslip; while the external domain changes for each condition (see Figure 2 for details). As only conditions without propeller effects are considered, the grid generated in the two volumes is imposed to be symmetric with respect to the symmetry plane of the aircraft model. This fact ensures that spurious differences resulting from a mesh effect are kept as low as possible, and it allows accurate comparison of the flow fields on the model skin and in the surrounding volume.

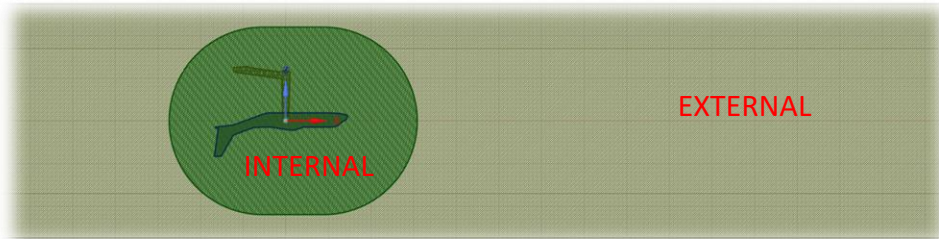


Figure 2: Details of INTERNAL and EXTERNAL domains

5 INTERFERENCE CALCULATIONS RESULTS

The strut effect is defined as the difference between the configuration with and the configuration without the strut at the same geometrical angle of incidence and sideslip:

$$\Delta C = C_{baseline} - C_{strut}, \quad (1)$$

$$\Delta \alpha = \Delta \beta = 0, \quad (2)$$

where C represents one of the aerodynamic forces and moments coefficients evaluated with respect to a body reference frame (i.e. C_x , C_y , C_z , C_{Mx} , C_{My} , C_{Mz}) and subscript indices *baseline* and *strut* refer to the configurations without and with the strut.

The correction of experimental data based on CFD results is derived by using two different approaches, i.e.

1. the generation of a polynomial surface as function of α and β ;
2. the generation of a fitting surface as function of α and β .

Both approaches allow the user to apply the correction to configurations in terms of α and

β which are not evaluated numerically. For every aircraft configuration and aerodynamic coefficient, it is necessary to generate a corresponding surface. The polynomial surfaces for all body axes coefficients in the cruise condition are presented in Figure 3. Figure 4 shows the fitting surfaces of the same configuration (see point 2).

The main result derived from Figure 3 and Figure 4 is that the corrections to be applied to experimental data and, then, the effect of the elliptic ventral strut on the global aerodynamic forces and moments are small. This aspect is especially evident for moderate α and β angles, while the corrections increase for conditions that are close to the border of the domain.

The polynomial fit gives smooth surfaces but they are not forced to pass through the original data points. This can lead to unacceptable errors at these points. Table 1 contains the values of the error quantity for each simulated α and β condition, i.e.

$$\Delta C_{CFD} - \Delta C_{POL}, \quad (3)$$

where ΔC_{CFD} is evaluated from original numerical data and ΔC_{POL} represents the same quantity derived from the polynomial surfaces. For the axial force (C_x) errors in the order of up 40 drag counts ($40e-4$) are observed. This is at least one order of magnitude larger than the accuracy expected from a wind tunnel test. This problem doesn't appear if an interpolation approach is used since it forces the surface through all the numerical points. For this reason, the actual correction is based on the second method, i.e. on the use of fitting surfaces. Figure 5 shows the comparison between original and corrected experimental data in terms of C_x , C_z and C_{My} for a cruise condition. As confirmed from the fitting surfaces, the correction applied to original experimental data is very small for all cases, demonstrating the controllable effect produced by the strut.

Table 1: Comparison between original and corrected numerical data ($\Delta C_{CFD} - \Delta C_{POL}$, cruise configuration)

α [°]	β [°]	C_x	C_y	C_z	C_{Mx}	C_{My}	C_{Mz}
-6.49	0	-2.79E-03	0	4.17E-04	0	-5.93E-04	0
0	0	-3.23E-03	0	1.64E-03	0	-8.91E-04	0
4	0	-1.73E-03	0	-8.01E-05	0	-2.77E-03	0
8	0	3.75E-03	0	-2.57E-03	0	2.96E-03	0
12	0	1.07E-02	0	5.22E-03	0	2.38E-04	0
-4	10	3.78E-04	-2.06E-06	2.43E-03	-1.49E-05	1.76E-03	5.47E-04
4	10	1.97E-03	-4.32E-06	2.61E-03	-4.42E-05	5.28E-03	1.64E-03
8	10	6.16E-03	1.91E-03	1.34E-02	-4.77E-04	-4.77E-03	-2.63E-04
0	15	4.96E-03	-4.72E-06	-1.22E-03	2.94E-04	-1.51E-03	1.20E-04
8	15	1.03E-02	-1.69E-03	2.04E-02	1.72E-04	1.93E-04	-1.80E-03
0	25	-2.29E-03	-9.19E-06	1.25E-02	-1.60E-04	-2.72E-04	-7.28E-04
8	25	1.76E-02	2.20E-04	6.12E-02	9.17E-05	4.34E-04	9.70E-04

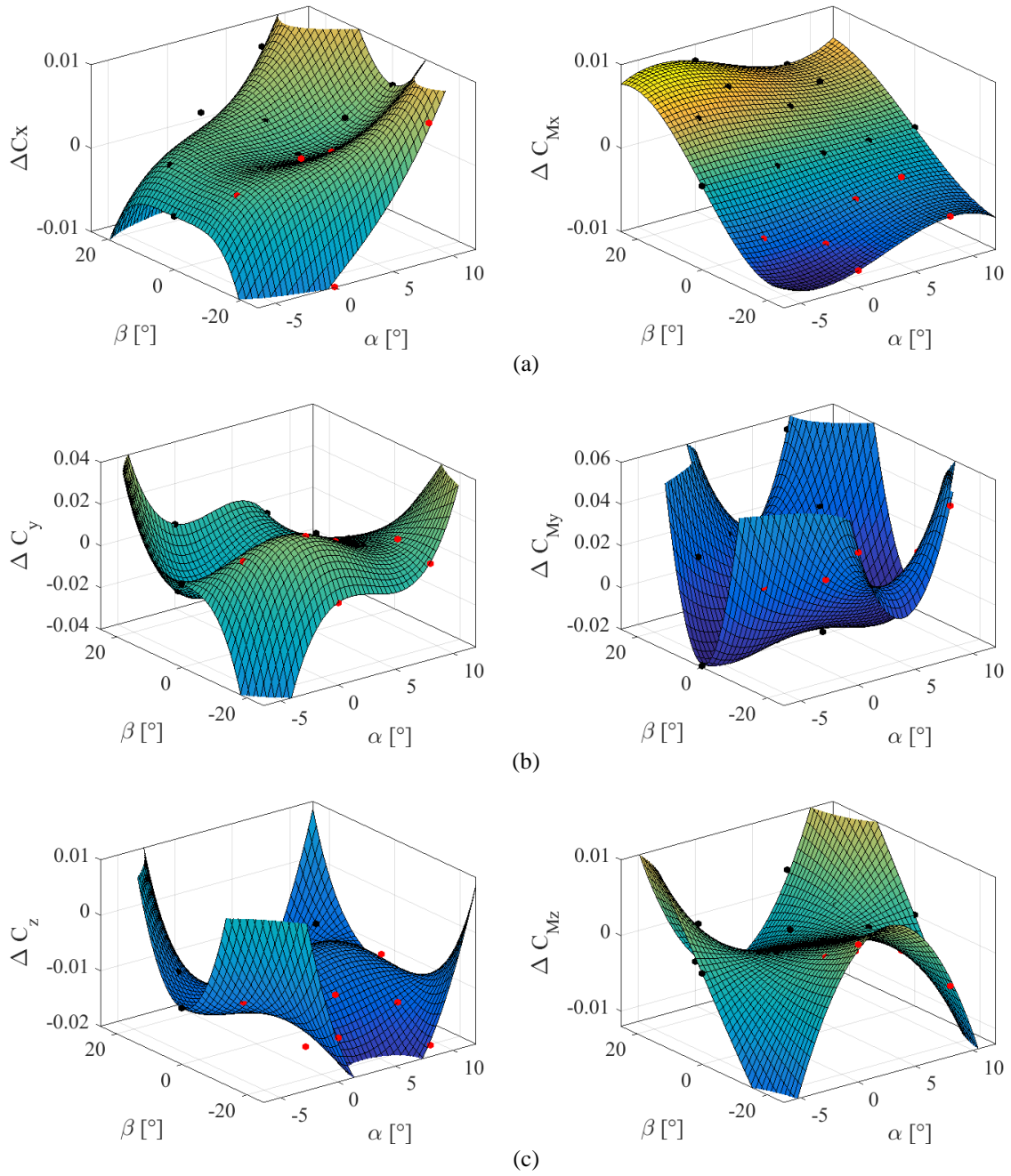


Figure 3: Polynomial surfaces (cruise configuration) for C_x and C_{Mx} (a), C_y and C_{My} (b), C_z and C_{Mz} (c)

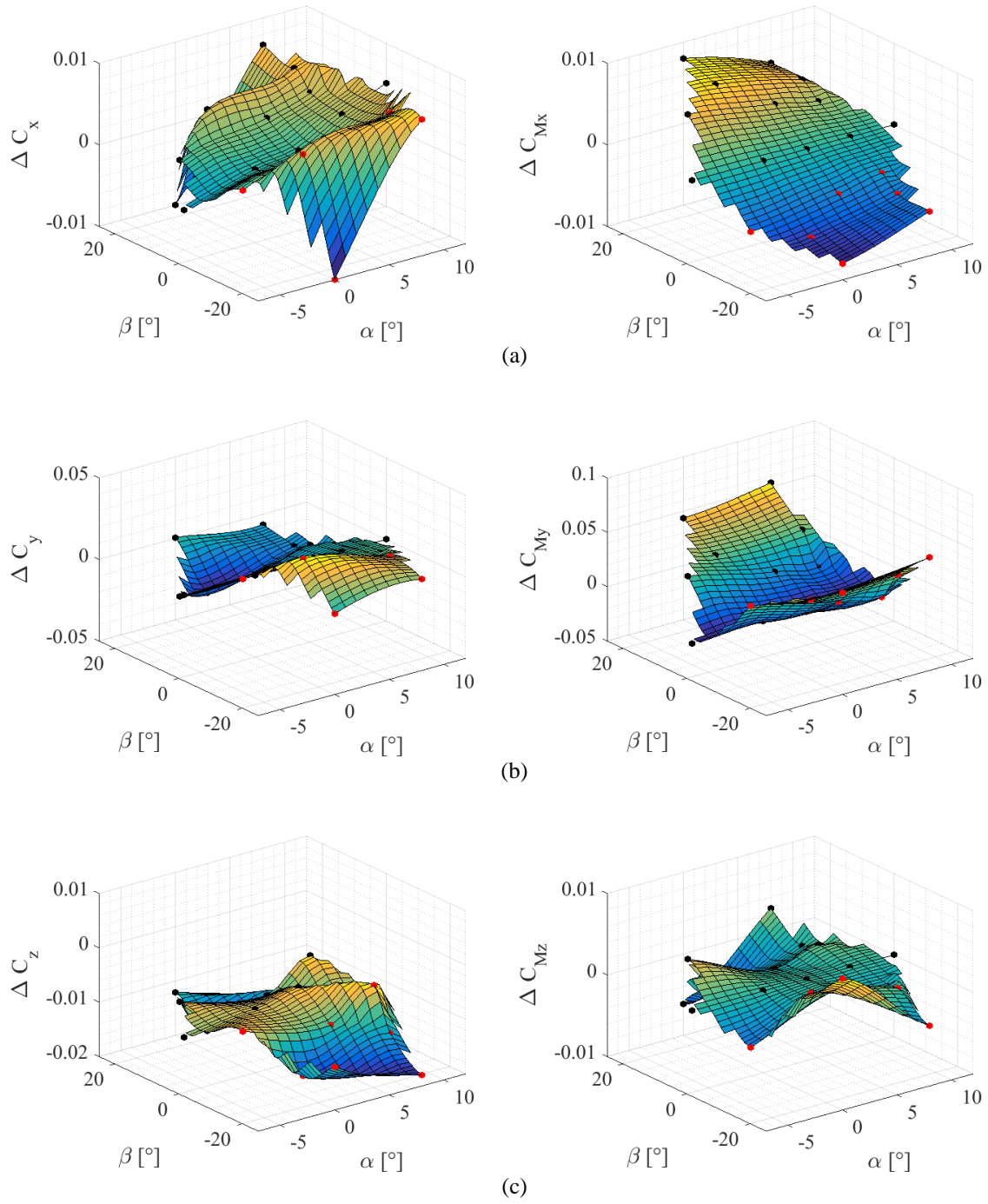


Figure 4: Fitting surfaces (cruise configuration) for C_x and C_{Mx} (a), C_y and C_{My} (b), C_z and C_{Mz} (c)

Figure 6 and Figure 7 depict, respectively, the polynomial and fitting coefficients ΔC_x , ΔC_z for the landing configuration. For this configuration, the same procedure of the cruise configuration is applied and, again, the fitting approach represents the most reliable one. By comparing Figure 6 with Figure 3 (and Figure 7 with Figure 4), it is possible to verify that the correction for the landing configuration differs from the same correction for cruise configuration, especially in the order of magnitude, demonstrating a greater effect of the elliptic strut in the high-lift condition. Even if the correction in this last case is more appreciable than the clean condition, it is possible to verify that the comparison between original and corrected experimental data shows that the effect of the strut remains small.

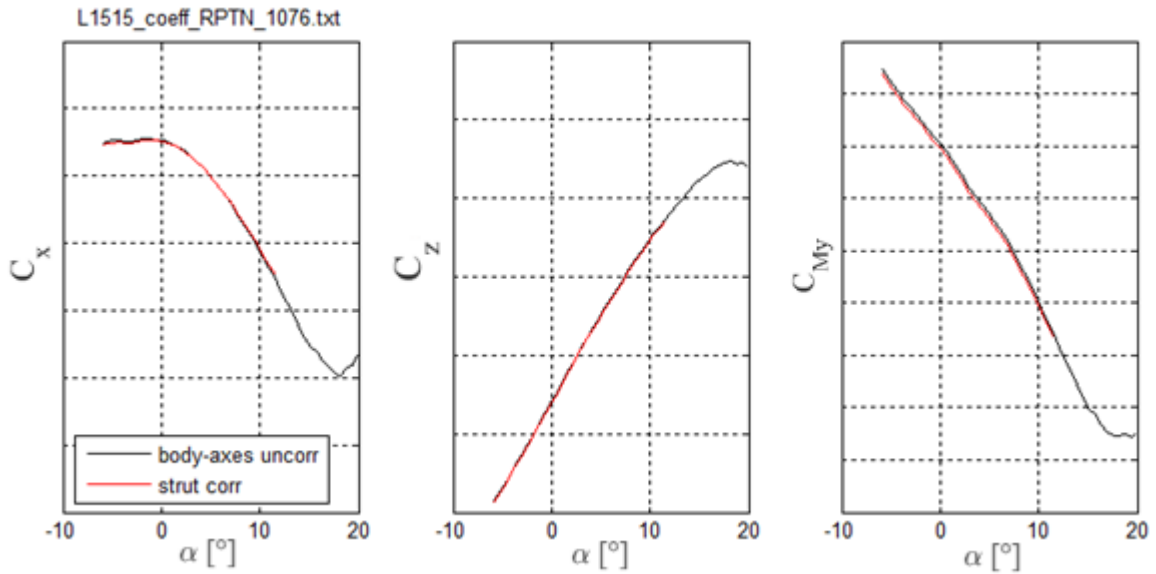


Figure 5: Original experimental data vs. Corrected experimental data (cruise configuration)

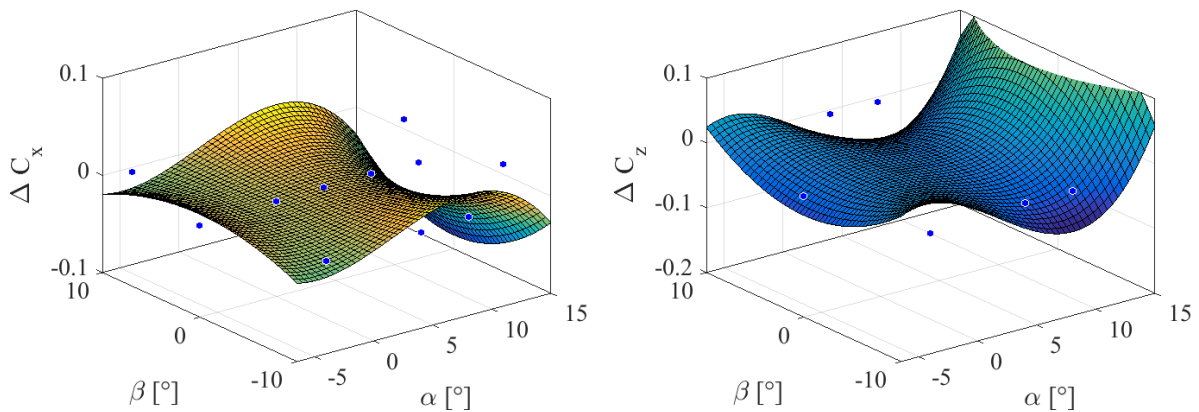


Figure 6: Polynomial surfaces (landing configuration) for C_x (left) and C_z (right)

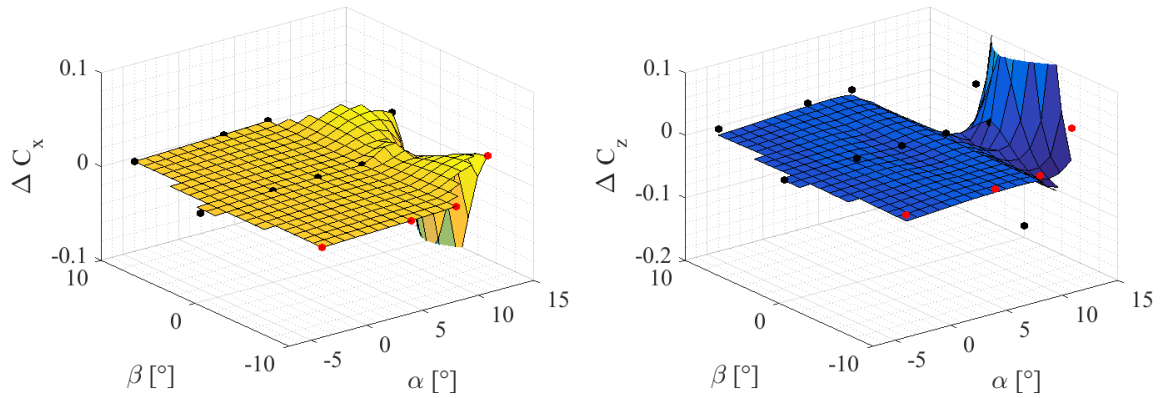


Figure 7: Fitting surfaces (landing configuration) for C_x (left) and C_z (right)

Figure 8 and Figure 9 show the comparison in terms of pressure coefficient distribution (C_p) between the configurations with and without the strut respectively for cruise and landing conditions. The distribution of pressure generated with the presence of the strut is very similar to the same in which the strut is not considered. The main differences are observable in the bottom part of the fuselage close to the intersection with the strut and they are more significant for the landing configuration. In any case, they produce only insignificant effects on the global aerodynamic coefficients.

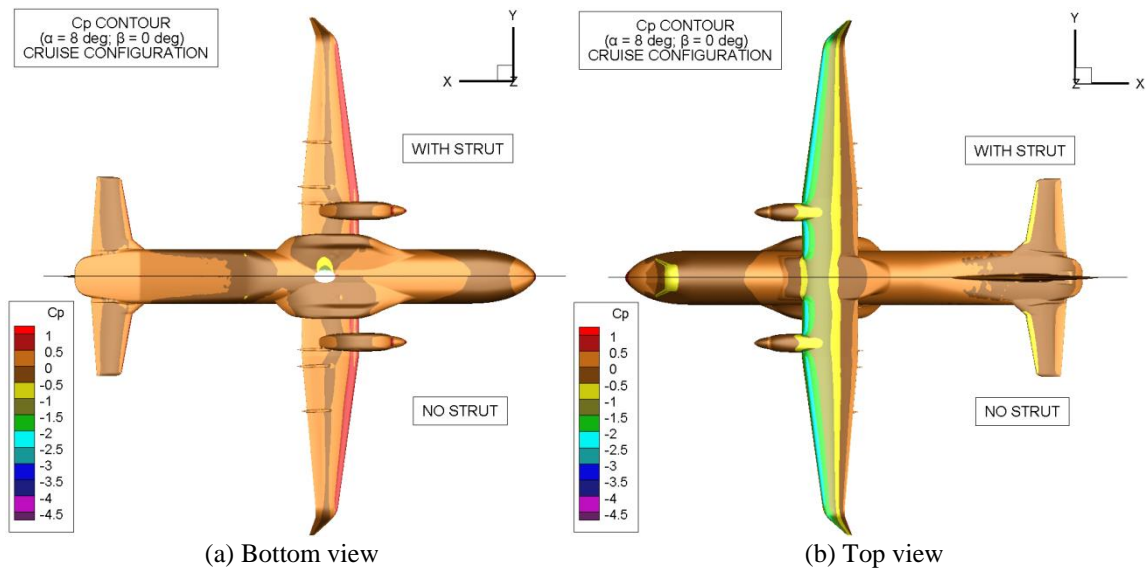


Figure 8: Comparison in terms of C_p contour distribution between the configurations with and without the strut (cruise conf. - $\alpha = 8$ deg, $\beta = 0$ deg)

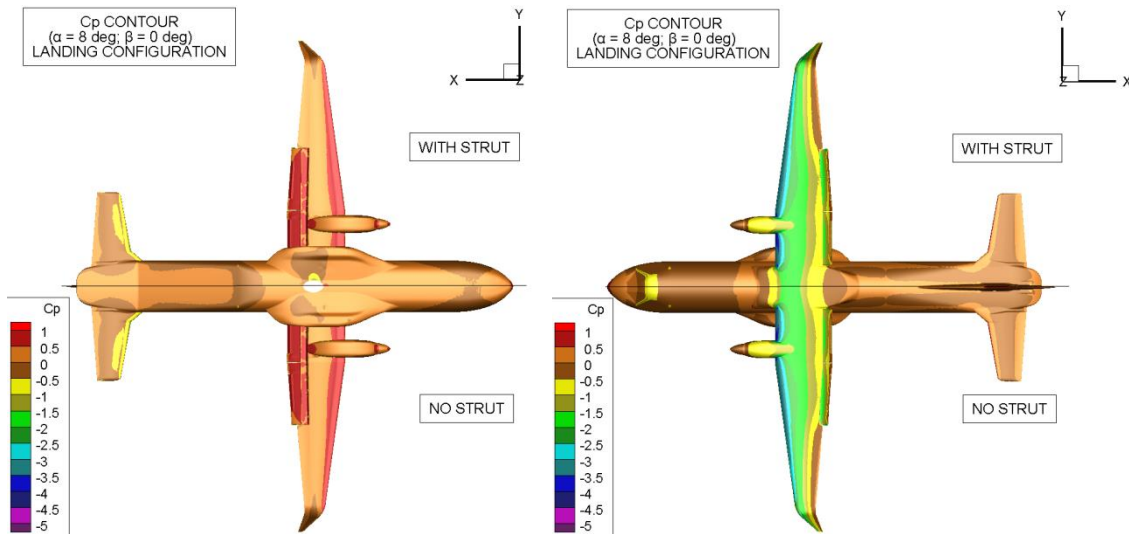


Figure 9: Comparison in terms of C_p contour distribution between the configurations with and without the strut (landing conf. - $\alpha = 8$ deg, $\beta = 0$ deg)

6 CONCLUSION

The aim of this study is the prediction of the effects of a single-strut interference on all aerodynamic forces and moments on an Airbus Defence & Space aircraft model tested in the RUAG Large Low Speed Wind Tunnel Emmen in Switzerland (LWTE). Two configurations of a scaled model of turboprop transport aircraft are addressed: the clean configuration representative of a cruise condition and a high-lift configuration with extended flaps, i.e. landing. RANS CFD simulations were used to predict the effect of a single strut on the global aerodynamic forces acting on the model.

The interference of the strut is evaluated by considering the difference between the configuration with and without the strut at the same geometrical angles of incidence and sideslip. The results are used to generate polynomial surfaces and/or interpolation surfaces for the correction of experimental data for each α and β . Polynomial surfaces were shown to produce excessive errors and it is recommended to use interpolated data for the actual corrections of experimental results.

The effect of the elliptic ventral strut on the global aerodynamic forces and moments was found to be small throughout the range of interest.

7 ACKNOWLEDGEMENT

The authors would like to thank the European Commission for funding part of this research work within the POLITE project.

REFERENCES

- [1] Zienkiewicz, O.C. and Taylor, R.L. *The finite element method*. McGraw Hill, Vol. I., (1989), Vol. II, (1991).
- [2] Idelsohn, S.R. and Oñate, E. Finite element and finite volumes. Two good friends. *Int. J. Num. Meth. Engng* (1994) **37**:3323-3341.

- [3] Lynch, F.T., Crites, R.C., Spaid F.W., *The crucial Role of Wall Interference*, Support Interference, and Flow Field Measurements in the Development of Advanced Aircraft Configurations, AGARD CP-535, (1993).
- [4] Elsenaar, A., Han, S.O.T.H., *A Break-Down of Sting Interference Effects*, NLR TP 91220 U, (1991).
- [5] Heidebrecht, A., *Simulation and Model Support Corrections for Slotted Wall Transonic Wind Tunnels*, AAAF Wind tunnel and computation: a joint strategy for flow prediction, FP20, AAAF, (2012).
- [6] Mouton, S., *Numerical Investigations of Model Support Interference in Subsonic and Transonic Wind Tunnels*, 8th ONERA-DLR Symposium ODAS 2007, Gottingen, October (2007).
- [7] Lyonnet, M., Piat, J.F., Roux, B., *Model Support Interference Assessment using a Metric Rear Fuselage and a Twin-Sting at ONERA S2MA Wind Tunnel*, International Conference on Experimental Fluid Mechanics, Turin, July 4-8, (1994).
- [8] Quest, J., *Tunnel Corrections in ETW*, ETW Technical Memorandum ETW/TM/99024, (1999).
- [9] Cartieri, A., Mouton, S., *Using CFD to calculate support interference effects*, 28th Aerodynamic Measurement Technology, Ground Testing, and Flight Testing Conference, AIAA 2012-2864, (2012).
- [10] Collercandy, R., Marquez, B., Lory, J., Dbjay, S., Espiau, L., *Application of CFD for Wall and Sting Effects*, HiReTT Technical Note HIRETT/TN/AF/RCo/WP2.2/3110, (2003).
- [11] Maina, M., Corby, N., Crocker, E.L., Hammond, P.J., Wong, P.W.C., *A Feasibility Study on Designing Model Support Systems for a Blended Wing Body Configuration in a Transonic Wind Tunnel*, The Aeronautical Journal, (2006).
- [12] Bush, R.H., Jasper, D.W., Parker, S.L., Romer, W.W., Willhite, P.G., *Computational and Experimental Investigation of F/A-18E Sting Support and Afterbody Distortion Effects*, Journal of Aircraft, Vol. 33, No. 2, (1996).
- [13] Müller, J., *Strut Interference Methodology and Results*, RUAG TB-TA-2740, 6.9.2016, internal RUAG document, (2016).
- [14] RUAG Aviations, *Capability Booklet Aerodynamics*, RUAG document, (2018).
- [15] van de Kreeke, M., Quémar, M., Verrière, M., *The Interference of the Model Support Mast with Measurements of the Longitudinal and Lateral Aerodynamic Coefficients*, NASA TT-20079, (1987).
- [16] Fluent 16.2 User's Guide, (2016).
- [17] ICEM User's Guide (2006).
- [18] Bardina, J.E., Huang, P.G., Coakley, T.J., *Turbulence Modelling Validation, Testing, and Development*, NASA Technical Memorandum 110446, (1997).